Physically-modeled 3D marine survey over HTI targets

Joe Wong

ABSTRACT

Using the University of Calgary Seismic Physical modeling Facility with a scale factor of 10^4, we conducted a high-resolution 3D marine survey over layered media containing HTI targets overlying a water-filled channel. The survey covered a scaled-up area of about 6000m by 6000m. Sources were placed on a rectangular grid with $\Delta X = \Delta Y =$ 100m. Receivers were placed on a rectangular grid with ΔX and ΔY = 50m. Source and receiver lines both were aligned in the Y direction. The minimum separation between source and receiver lines was 100m. The data were digitized with 2ms sampling and 14-bit precision. Seismograms with length of 2000ms were recorded with vertical stacking of 200 repeated waveforms and stored in SEG-Y files. To reduce survey time, acquisition was conducted using eight simultaneous sources. The resulting supergathers of seismic traces must be deblended or separated into ordinary common source gathers before further post-survey processing and imaging.

INTRODUCTION

A scaled-down 3D marine survey was conducted over the four-layer physical model depicted on Figures 1 and 2. The survey generated three large SEG-Y files:

H2O_PVC_PUCK_CHAN_Sep_16_2013.sgy,
H2O_PVC_PUCK_CHAN_Sep_17_2013.sgy,
H2O_PVC_PUCK_CHAN_Oct_01_2013.sgy.

These files hold seismic data acquired over two different regions of the physical model. The Sep_16 and Sep_17 files focus on the area defined approximately by (-3000m $\leq Y \leq$ 0m). These two files may have some small overlap in the coverage of the survey area. The Oct_01 file focuses on the area defined by (0m $\leq Y \leq$ 3000m). The information from the two areas files can be processed and analyzed as if they were from different surveys, or they can be combined to be treated as information from a single survey.

In order to complete the survey in a reasonable length of time, the seismic data were acquired using eight simultaneous sources. Every trace in the dataset is a supertrace, that is, it contains arrivals from eight sources. There are over 830,000 supertraces in the dataset. The information content in the dataset is equivalent to that from about 6.6 million ordinary traces (an ordinary traces contain arrivals from only one source),

Before further processing, the supergathers of blended seismic data generated by eight simultaneous sources must be separated to yield eight ordinary common source gathers (CSGs). The shifted-apex deblending algorithm (Trad et al., 2012) is a good candidate for separating the supergathers from this physical modeling experiment.

To reduce the computation burden of additional processing and reflection imaging, the sizes of the deblended datasets can be reduced by ignoring all seismograms with source-receiver offsets larger than 1000m or CMP coordinates outside the range -2800m $\leq X_{mid}$,

$Y_{mid} \leq 2800$m. The sizes of the deblended datasets can be reduced further by truncating the lengths of all seismograms from 2000ms to 1200ms, since there is no useful reflection information at times greater than 1200ms.

The information resulting from deblending and limiting the two files can be processed and imaged separately, or they can be combined and treated as a single dataset. The main task is to image the tops of the HTI pucks beneath the PVC layer. A second task is to image the bottoms of the HTI pucks. A final and much more difficult task is to image the water-filled channel beneath the HTI pucks.

Another important goal of analyzing the data from this 3D marine survey is to extract AVAZ information and map the directions of the "fracture orientations" or symmetry axes within the different HTI pucks. Also, the extracted AVAZ information can be inverted using Rüger's formulas to estimate the Thomsen's parameters for the VTI/HTI anisotropy. In order to do AVAZ analysis properly, the deblending method must preserve the true relative amplitudes of the reflections.

MODEL DESCRIPTION

The model consists of a PVC layer overlying a Plexiglas (PLX) layer with embedded HTI cylinders of various sizes (the "PUCK" layer), overlying another Plexiglas layer with an open channel (the "CHAN" layer). Top views of the PUCK and CHAN layers are shown on Figure 1. All three layers were immersed in water, and a 3D marine survey was conducted over the resulting four-layer model.

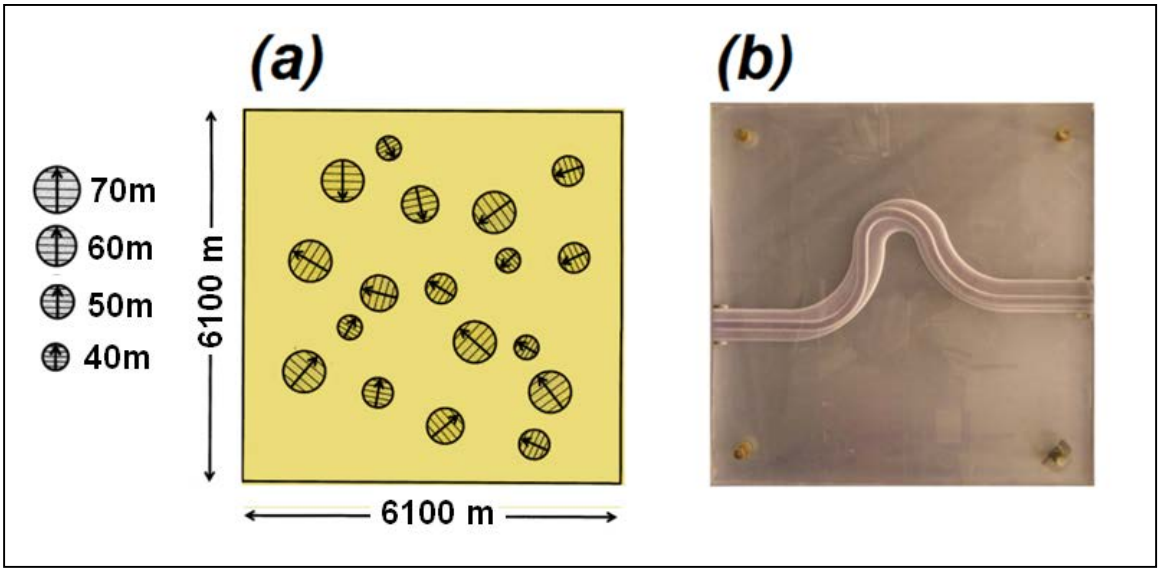

FIG. 1. (a) Top view of the Plexiglas layer with embedded HTI targets ("PUCK" layer). (b) Top view of the Plexiglas layer with a cut channel ("CHAN" layer). The HTI pucks are short 250-m-thick cylinders of anisotropic Phenolic LE laminate material. The arrows indicate the symmetry axes for the various HTI pucks. Plexiglas is the trade name for acrylic plastic.

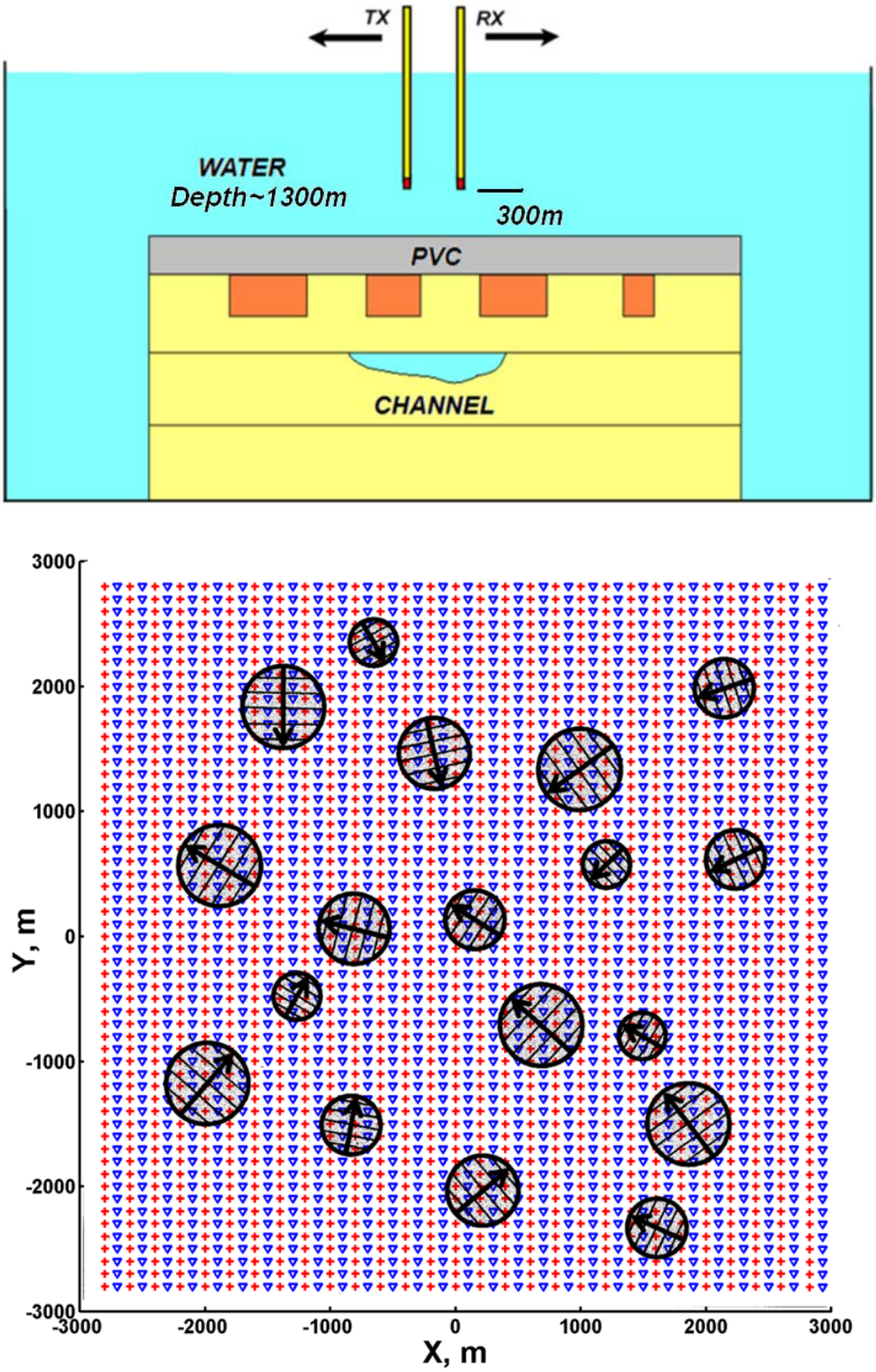

FIG. 2. Schematic side and top views of acquisition geometry for the marine 3D survey over the model. Upper diagram: the HTI cylinders or "pucks" are shown in light-brown; the yellow material is Plexiglas (PLX). Table 1 lists the physical properties of the various materials. Source (TX) and receiver (RX) transducers are Dynasen CA-1136 piezopins.

Figure 2 shows schematically the side and top views of the model and the acquisition geometry for the 3D survey. The thickness of the PVC layer is about 250m ±5m. The thickness of the HTI pucks is about 250m ±5m. The distance between the top of the HTI pucks and the top of the cut channel is about 480m ±5m. The thickness of the cut channel varies, but has a maximum value of about 250m.

The red crosses shown on the top view are source locations; blue triangles are receiver positions (only every second receiver is shown). The arrows indicate the symmetry axes of the HTI pucks located beneath the PVC layer. The strike of the hidden channel beneath the pucks is generally in the X direction. The water-PVC interface is not perfectly horizontal; it dips downwards slightly as the x coordinate increases.

TABLE 1. Physical properties of the materials in the Water-PVC-Puck-Channel model. The two velocity values listed for HTI pucks are the fast and slow velocities for Phenolic LE material. Approximate uncertainties in velocities and densities are ±50 m/s and ±50 kg/m^3, respectively.

Material	P-Wave Velocity, m/s	S-Wave Velocity, m/s	Density, kg/m^3
Water	1485	0	1000
PVC	2350	1080	1380
HTI Pucks	3600, 2850	1650, 1550	1390
PLX	2750	1375	1190

.

SEG-Y FILES GENERATED BY USING SIMULTANEOUS SOURCES

Table 2 lists three files generated by the 3D survey. Each file contains data from a different sub-region of the complete covered area. There may be a small amount of overlap between the Sep_16 and Sep_17 files.

TABLE 2. Files generated by the 3D marine survey.

SEGY File Name	(Dx , Dy) Spacings, m	Number of Traces	Time, hours
H2O_PVC_PUCK_CHAN_Sep_16_2013.sgy	Tx: (100, 100) Rx: (50, 50)	23.780	15.5
H2O_PVC_PUCK_CHAN_Sep_17_2013.sgy	Tx: (100, 100) Rx: (50, 50)	391,000	254
H2O_PVC_PUCK_CHAN_Oct_01_2013.sgy	Tx: (100, 100) Rx: (50, 50)	418,600	270

In conducting the 3D survey, we used a single receiver piezopin transducer (Dynasen CA-1136) and a source array consisting of eight piezopin transducers (also Dynasen CA-1136). Adjacent transducers in the source array were separated by 400m and aligned in the Y-direction. To speed up acquisition so that the 3D survey could be completed in a reasonable number of days, the eight sources were fired simultaneously, so that each recorded seismogram is a super trace. Many super traces from many receiver positions but associated with a single source array position form a supergather. The first step in processing a dataset recorded with simultaneous sources is "deblending", i.e., the separation of supergathers into ordinary common source gathers (CSGs). This must be done before the application of standard processing and imaging techniques.

In standard SEG-Y files, the SRCX and SRCY headers give the source coordinates (multiplied by 10) of each seismogram, while the GRPX and GRPY headers give the receiver coordinates (multiplied by 10). The files in Table 2 were recorded using simultaneous sources, so the SRCX and SRCY headers give only the Y coordinates of the first source in the array of eight sources. After deblending each supergather into eight separate ordinary CSGs, the SRCY coordinates of the CSGs after the first one must be re-assigned correct values, either by using the observed y-coordinates of the hyperbolic apexes, or by sequentially adding 4000 (400m times 10). True positions of the sources may deviate from the header coordinates by as much as ±20m (experimental error).

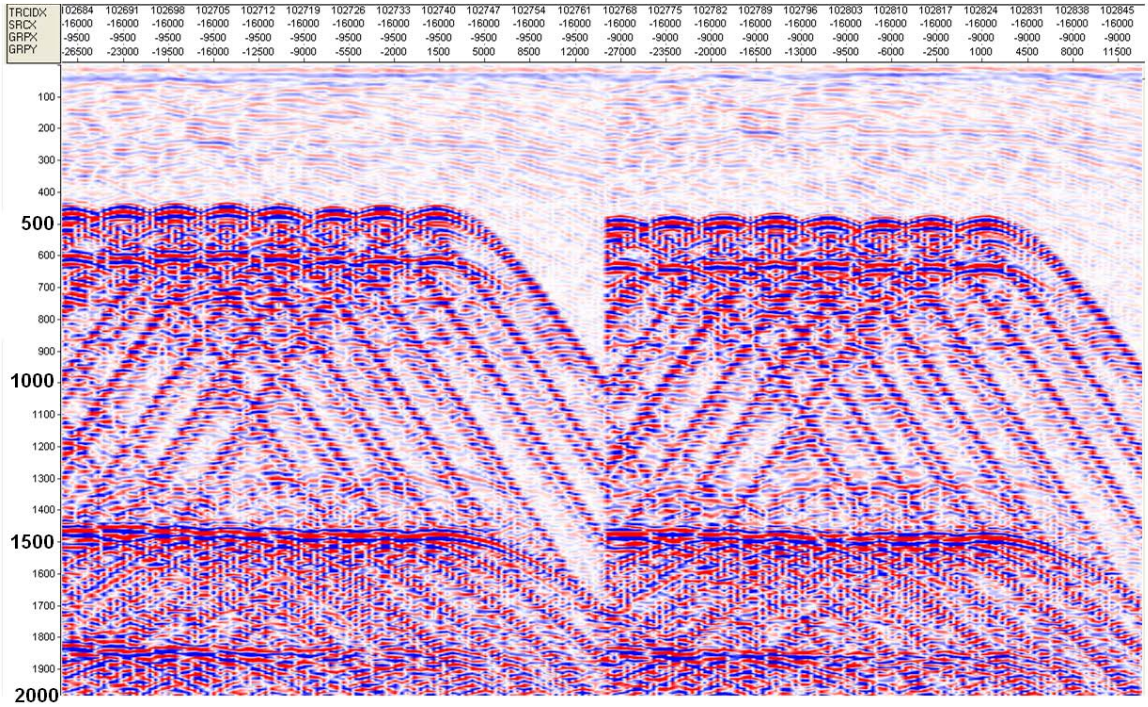

FIG. 3. AGC plot of two supergathers from the Sep_17 file. Source line location SRCX = -1600m; receiver line locations are GRPX = -950m (left) and GRPX = -900m (right). The receiver coordinates GRPY vary from -3000m to 1500m. The SRCX, GRPX, and GRPY header values written in the file (and shown along the top of the plot) must be divided by 10 to get meters. The vertical axis is time in milliseconds.

EXAMPLE SUPERGATHERS

The utility program SeiSee.exe was used to plot the seismogram gathers shown on Figures 3 to 7. SeiSee.exe is free software that can be downloaded from the link obtained by entering "SeiSee Download" in a Google search.

The numbers shown along the top of the plots are SEG-Y headers. The TRCID header is the trace number within each file. The SRCY coordinates of the source array vary from -3000m to 1500m.; they are nor shown on the plots but will be found in the SEG-Y trace headers. The SRCX, GRPX, and GRPY header values written in the files and shown along the top of the plot must be divided by 10 to get meters.

Figure 3 is an AGC plot of two supergathers for source line location SRCX = -1600m. The times at the apexes of the topmost hyperbolas (approximately 438ms for the left set and 471ms for the right set) are equal to the distances between the source and receiver lines (650m and 700m) divided by the water velocity (1485m/s). The strong reflection at about 1450ms and 1820ms are reflections due to the presence of the water-air interface about 1000m above the active tips of the piezopin transducers (see Figure 2). These events are of no interest to us, as they are not related in any way to the HTI and channel targets. The reflection event from the water-PVC interface occurs at about 590ms to 610ms. The events of most interest are reflections from the top of the HTI pucks. After the supergathers on Figure 3 are deblended, the apexes of the reflection hyperbolas associated with the HTI pucks should appear at times between 740ms and 780ms on the CSGs.

Figures 4 to 7 are AGC plots of other example supergathers from the 3D survey. The header values at the top of the plots and the numbers on the time axis can be more easily seen if the pictures are zoomed to get expanded views.

Three kinds of events can be seen clearly on Figures 4 to 7. The earliest-arriving hyperbolas, with apexes at about 70ms to 250ms, are the direct arrivals through water. The hyperbolas just below, with apexes at about 400mms to 500ms, are reflections from the water-PVC interface. The third set of hyperbolas, with apexes between 600ms and 800ms, are the reflections from the top of PUCK layer. The events near 1000ms showing poor spatial coherence possibly are reflections from the interface between the PUCK layer and the CHAN layer.

SUGGESTIONS FOR PROCESSING AND IMAGING

For processing and analysis, the entire Sep_16 file can be ignored, as it was recorded only as a test.

The Sep_17 file and the Oct_01 file should be considered as separate datasets. Before standard processing and migration techniques can be applied, the supergathers must be separated to obtain ordinary common source gathers (CSGs). This process is known as deblending. The deblended CSGs from these two files should be stored in separate SEG-Y files, and all subsequent processing, analysis, and imaging of the deblended data should be done separately. Different statics corrections must be used for the reflections in the two datasets (due to the dipping water-PVC interface).

Deblending algorithms have been described by many authors (Abma et al., 2012; Henley, 2014; Mahdat et al., 2011; Cheng and Saachi, 2013). The shifted-apex method described by Trad et al. (2012) seems to be particularly useful for deblending the data described in this report.

Every effort must be taken to preserve true relative amplitudes in the deblending procedure in order that AVAZ analysis can be done on the deblended data. In this regard, it may be noted that one piezopin source is discernibly weaker that the other sources in the array (easily seen as the third one from the left on Figure 7). The relative amplitudes of all traces in the deblended common source gathers must be calibrated and balanced. This is done by normalizing all traces associated with each source using the (averaged) amplitude of the direct water arrival(s) on the trace(s) with the minimum arrival time(s) for that source

Before saving the processed data in new SEG-Y files, the deblended seismograms can be truncated from 2000ms to 1200ms, since no useful reflections appear after 1200ms. In addition, we can ignore seismograms with source-receiver offsets greater than 1000m or with source-receiver midpoints outside the ranges (-2800m ≤ X, Y ≤ 2800m). By limiting the deblended data in this way, we significantly reduce the sizes of the datasets to be further analyzed, and imaged.

DEBLENDING USING APEX- SHIFTED HYPERBOLA

A 3D supergather of traces can considered as a sum of events with hyperbolic moveout in space-time domain:

$$D(x,t) = \sum d_i(x,t,\tau_i,v_i,h_i)\ , \tag{1a}$$

$$t = sqrt[\tau_i^2 + (x-h_i)^2/v_i^2]\ , \tag{1b}$$

where (τ_i, v_i, h_i), i = 1, 2,… n , are time, velocity, and offset parameters describing a finite number of hyperbolic trajectories in space-time domain. Trad (2003) combined these two equations with a sparse-inversion algorithm to create the apex-shifted Radon transform (ASRT), which was used by Trad et al. (2012) to approximate supergathers by sets of common source gathers to a high degree of accuracy.

Wong (2012) used the same equations iteratively to separate an eight-source supergather from a physical-model marine survey into individual common source gathers. Beginning with the shallowest events and proceeding to the deepest events, the method essentially consisted of flattening hyperbolic events and filtering in wavenumber domain to isolate the flatten events.

Henley (2014; this volume) used iterative radial-trace filtering targeted on shifted hyperbolic apexes to deblend supergathers acquired in a physically-modeled 3D survey. He investigated how the spacing between simultaneous sources and the distance between parallel source and receiver lines affected the effectiveness of the method.

CONCLUSION

Acquisition in 3D surveys is much more efficient when multiple seismic sources are activated simultaneously. The multi-sourcing technique results in supergathers of supertraces. On such supergathers, the seismograms for a given receiver contain arrivals from all the simultaneous sources.

On Table 2, we see that it took 537 hours (about 22 days) of continuous recording to cover the entire 6000m by 6000m area and complete the survey. If the survey had been conducted using sequential instead of simultaneous sources, it would have taken at least eight times longer, more than 5 months, to acquire the same information. Such long acquisition times are impractical, and would make physical modeling of high resolution 3D surveys highly unappealing.

A main goal of processing the physical-modeled seismic data in this report is the creation of a 3D image of the HTI pucks. A more challenging goal is to image the water-filled channel beneath the HTI pucks.

We also may be able to obtain important attributes related to the HTI anisotropy of the Phenolic pucks by analyzing AVAZ effects using the Rüger equations (Rüger, 1998; Mahmoudian, 2013; Mahmoudian et al., 2014). Two such attributes are ε, the ratio of fast to slow P-wave velocities, and ϕ_0, the direction of the symmetry axis relative to the X-axis. AVAZ analysis requires that the deblending process preserves the true relative amplitudes of the reflections.

ACKNOWLEDGEMENT

We thank the industrial sponsors of CREWES and NSERC (Natural Sciences and Engineering Research Council of Canada) for supporting this research.

REFERENCES

Abma, R., Zhang, Q., Adeyemi Arogunmati, A., and Gerard Beaudoin, G., 2012. An overview of BP's marine Independent Simultaneous Source field trials: SEG Technical Program Expanded Abstracts, pp. 1-5. doi: 10.1190/segam2012-1404.1

Beasley, C., 2008. A new look at marine simultaneous sources, The Leading Edge, **27**, 914-917.

Bouska, J., 2010. Distance separated simultaneous sweeping for fast clean vibroseis acquisition, Geophysical Prospecting., **58**, 123-153.

Cheng, J., and Sacchi, M., 2013. Separation of simultaneous source data via iterative rank reduction: SEG Technical Program Expanded Abstracts, pp. 88-93. doi: 10.1190/segam2013-1313.1

Henley, D. and Wong, J., 2014. Reversing entropy: de-blending and processing physical model data, CREWES Research Report, this volume..

Mahdad, A., Doulgeris, P., and Blacquiere, G., 2011. Separation of blended data by iterative estimation and subtraction of blending interference noise: Geophysics, **76**(3), Q9-Q17. doi: 10.1190/1.3556597

Mahmoudian, F., 2013. Physical modeling and analysis of seismic data from a simulated Fractured medium (Chapter 4): Ph.D. Thesis, University of Calgary.

Mahmoudian, F., Margrave, G., Wong, J., and Henley, D., 2015. Azimuthal AVO analysis of physical modeling data acquired over an azimuthally anisotropic medium: Geophysics, in press.

Rüger, A., 1998. Variation of P-wave reflectivity with offset and azimuth in anisotropic media: Geophysics, **63**, pp. 935-947. doi: 10.1190/1.1444405

Trad, D., Siliqi, R., Poole, G., and Boelle, J., 2012. Fast and robust deblending using Apex Shifted Radon transform: SEG Technical Program Expanded Abstracts, pp. 1-5. doi: 10.1190/segam2012-0703.1

Trad, D., 2003. Interpolation and multiple attenuation with migration operators: Geophysics, **68**, p.2043–2054

Wong, J., 2013. Seismic physical modeling I: acquisition of 2D and 3D surveys involving HTI targets: CREWES Research Report 25, pp. 82.1-82.12.

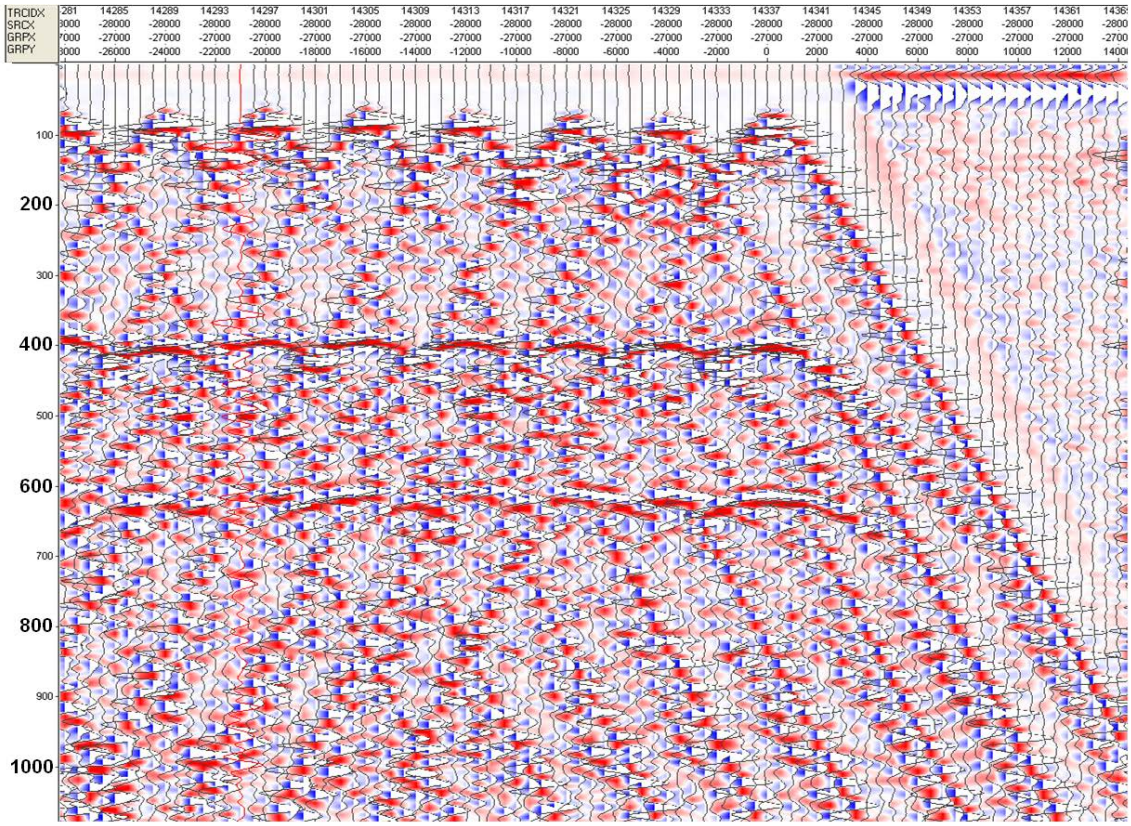

FIG. 4. Supergather from file H2O_PVC__PUCK_CHAN_Sep_17_2013.sgy. Traces are separated by ΔY=50m, and run from Y=--2800m to Y=1400m. The Y coordinates of the source points for the hyperbolas from left to right are -2800m, -2400m, -2000m, -1600m, -1200m, -800m, -400m, and 0m, respectively. The X coordinate of the source line is -2800m, while the X coordinate of the receiver line is -2700.

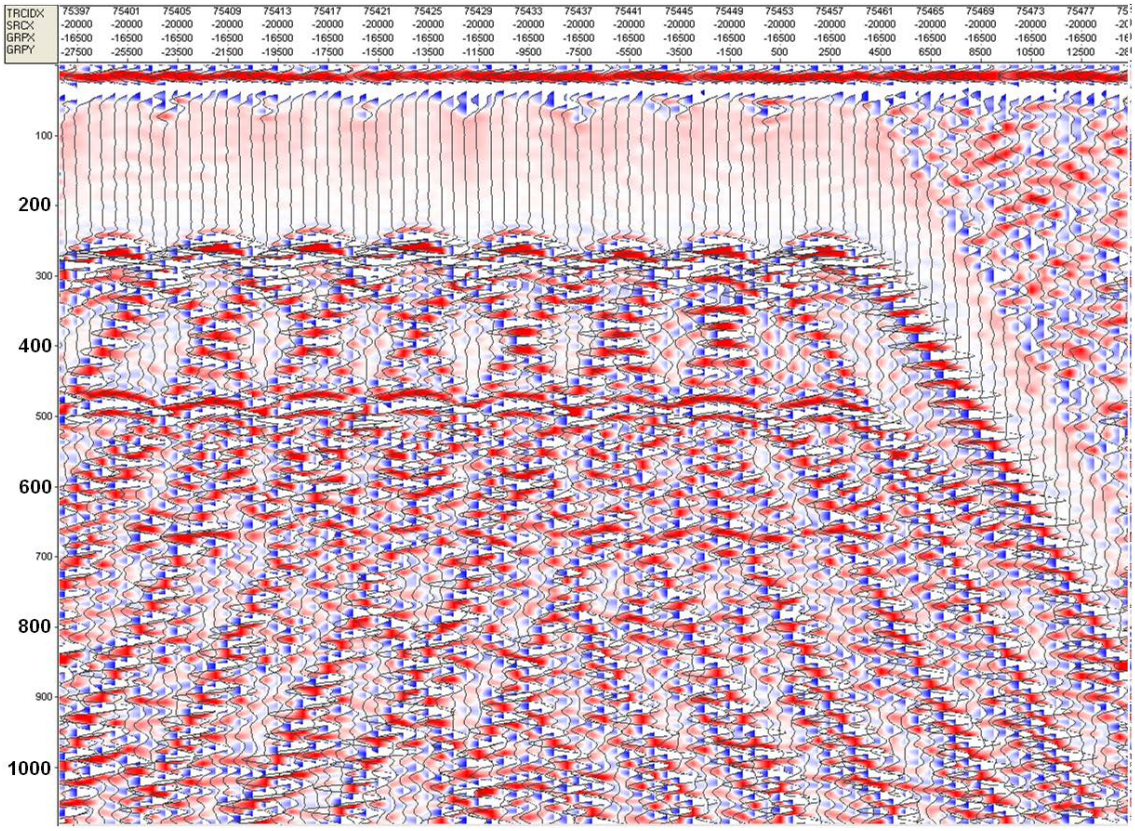

FIG. 5. Supergather from file H2O_PVC__PUCK_CHAN_Sep_17_2013.sgy. Traces are separated by ΔY=50m, and run from Y=--2800m to Y=1400m. The Y coordinates of the source points for the hyperbolas from left to right are -2600m, -2200m, -1800m, -1400m, -1000m, -600m, -200m, and 200m, respectively. The X coordinate of the source line is -2000m; the X coordinate of the receiver line is -1650m.

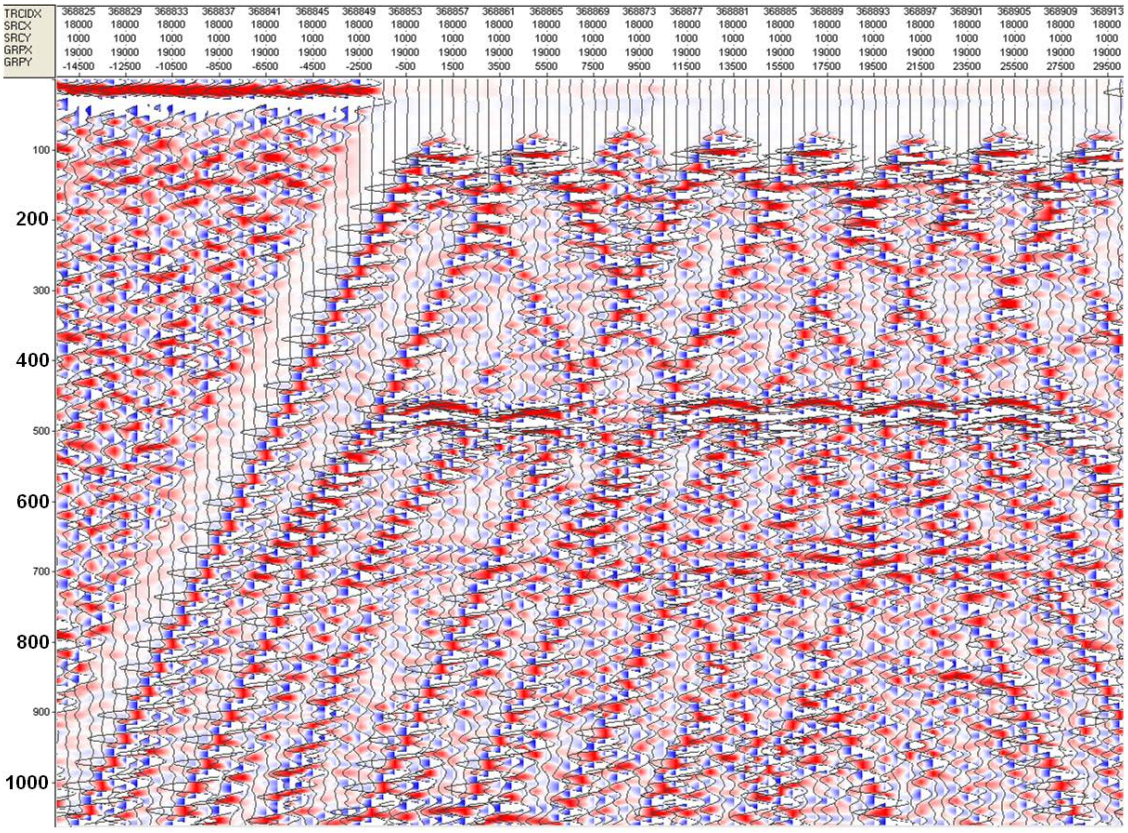

FIG. 6. Supergather from file H2O_PVC__PUCK_CHAN_Oct_01_2013.sgy. Traces are separated by ΔY=50m, and run from Y=-1500m to Y=3000m. The Y coordinates of the source points for the hyperbolas from left to right are 100m, 500m, 900m, 1300m, 1700m, 2100m, 2500m, and 2900m, respectively. The X coordinate of the source line is 1800m; the X coordinate of the receiver line is 1900m.

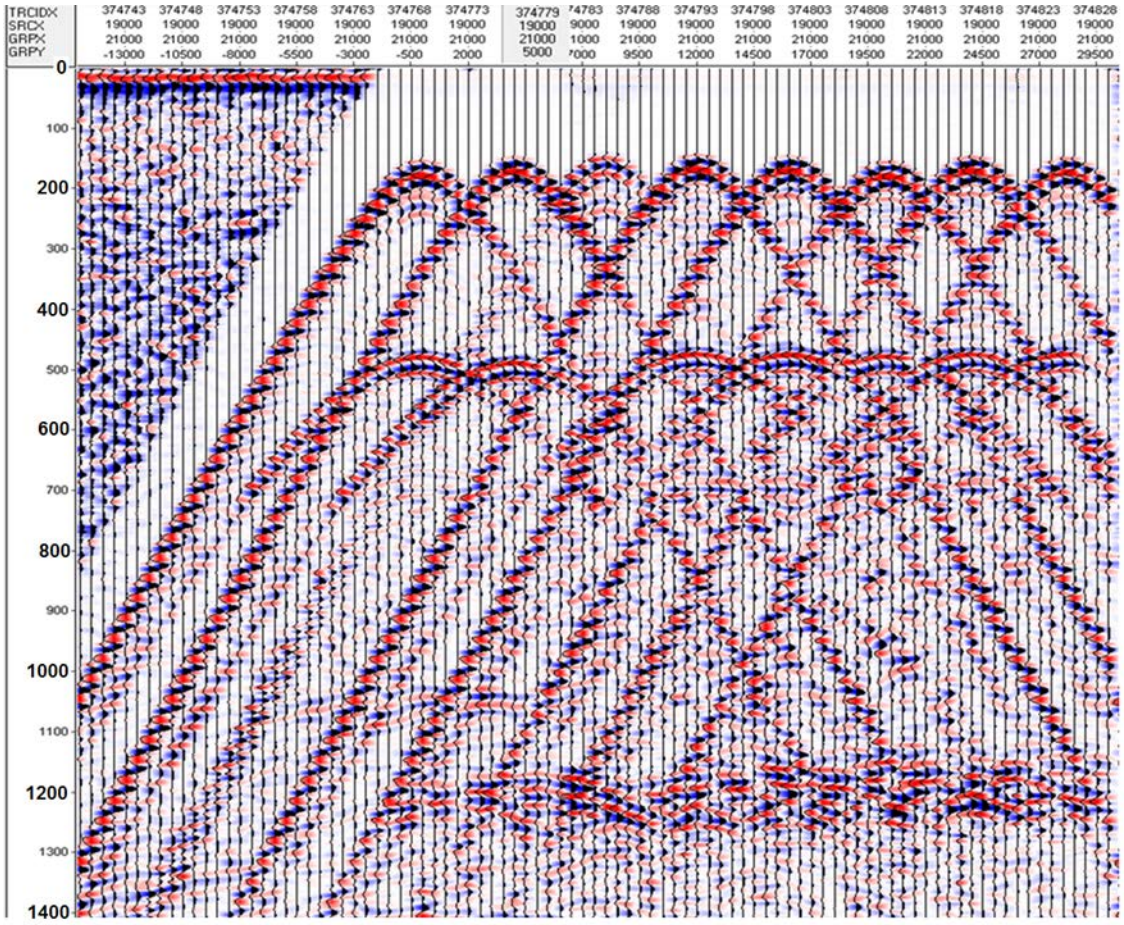

FIG. 7. Supergather from file H2O_PVC__PUCK_CHAN_Oct_01_2013.sgy. Traces are separated by ΔY=50m, and run from Y=-1500m to Y=3000m. The Y coordinates of the source points for the hyperbolas from left to right are 0m, 400m, 800m, 1200m, 1600m, 2000m, and 2400m, respectively. The X coordinate of the source line is 1900m; the X coordinate of the receiver line is 2100m.